



PV CELL MODULE MODELING & ANN SIMULATION FOR SMART GRID APPLICATIONS

ADEL EL SHAHAT

Research Scientist, Mechatronics-Green Energy Lab., Elect. & Comp. Eng. Dept., OSU, USA, 43210

E-mail: adel.elshahat@ieee.org, ahmed.210@osu.edu

ABSTRACT

This paper proposes general and specific modeling and simulation for Schott ASE-300-DGF PV panel for Smart Grid applications. This is done, with the aid of MATLAB environment and Artificial Neural Network (ANN). First modeling of PV cell module at nominal conditions at 25°C, and 1KW/m² with I-V curves at (0°C, 25°C, 50°C, 75°C), also power and irradiance. Then, we propose general modeling and simulation at more probable situations for variable values of temperature and irradiance. The simulation results at each irradiance value with various temperature values and corresponding characteristics are well depicted in 3-D figures. Later, the ANN model for the proposed range of irradiance and temperature as model inputs, with the corresponding values of voltages, currents, and power as outputs is presented. Finally, algebraic equations for the ANN model are deduced.

Keywords: *Modeling, Simulation, Smart Grid, MATLAB, Neural Network, PV Cell.*

1. INTRODUCTION

Due to the importance of PV cell especially in Smart Grid Energy Systems (SGES) this paper is proposed. Smart Grid Energy Systems (SGES) is recently increasing, particularly onsite generation. This interest is because larger power plants are economically unfeasible in many regions due to increasing system and fuel costs, and more strict environmental regulations. In addition, recent technological advances in small generators, Power Electronics, and energy storage devices have provided a new opportunity for distributed energy resources at the distribution level [1-3]. Photovoltaic systems have become increasingly popular and are ideally suited for distributed systems. Many governments have provided the much needed incentives to promote the utilization of renewable energies, encouraging a more decentralized approach to power delivery systems. In spite of their relatively high cost, there has been very remarkable growth in installed Photovoltaic systems. Recent studies show an exponential increase in the worldwide installed photovoltaic power capacity. There is ongoing research aimed at reducing the cost and achieving higher efficiency. Furthermore, new regulatory laws mandating the use of renewable energy have expanded this market

around the world. Currently, photovoltaic generation systems are actively being promoted in order to mitigate environmental issues such as the green house effect and air pollution. Solar energy is the world's major renewable energy source and is available everywhere in different quantities. Photovoltaic panels do not have any moving parts, operate silently and generate no emissions. Another advantage is that solar technology is highly modular and can be easily scaled to provide the required power for different loads [4], [5]. The fuel cell was invented by Sir William Grove in 1839, but was not used in a practical application until proton-exchange membrane fuel cells (PEMFCs), made by General Electric, were employed in the National Aeronautics and Space Administration (NASA) Gemini missions in the early 1960s. As a result, the Alkaline Fuel Cell (AFC) was used for a time by NASA, and the use of PEMFCs became almost non-existent. In the 1990s, the PEMFC regained its status as the dominant fuel cell type, and fuel cells in general have received considerable attention as an alternative to fossil fuel combustion. Much of the credit for the revitalization of the PEMFC must be given to Ballard Power Systems and to the Los Alamos National Laboratory. The PEMFC is now seen by many researchers and companies as the only fuel cell type suitable for

vehicular applications, due to a relatively high power density, low operating temperature and solid electrolyte. A significant amount of fuel cell research focuses on fundamental issues of performance and cost [6-9]. And finally, some of recent research advances examples about this topic are introduced in [10-12]. This paper introduces general and specific modeling and simulation for Schott ASE-300-DGF PV panel [13] for Smart Grid (SG) applications as shown in figure [1].

cell manufacture is mono – crystalline or poly – crystalline silicon. Each cell is typically made of square or rectangular wafers of dimensions measuring about 10 cm × 10 cm × 0.3 mm. In the dark, the PV cell’s behavior is similar to that of a diode and the well known Shockley-Read equation can be [1], [14].

3. ASE-300-DGF PV MODULE

The ASE-300-DGF/50 is an industrial-grade solar power module built to the highest standards. Extremely powerful and reliable, the module delivers maximum performance in large systems that require higher voltages, including the most challenging conditions of military, utility and commercial installations. For superior performance, quality and peace of mind, the ASE-300-DGF/50 is renowned as the first choice among those who recognize that not all solar modules are created equal [13].

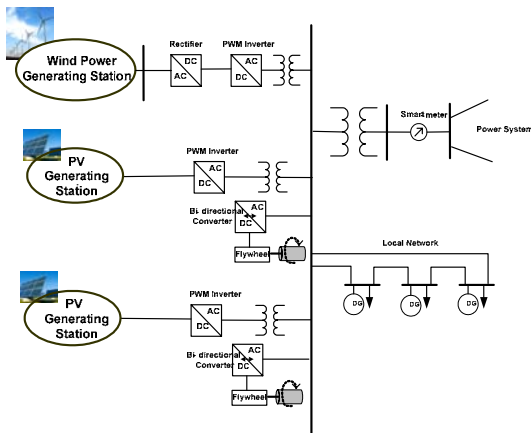


Figure 1: Simple Smart Grid System with PV Generating Station [1].

2. PV CELL

A commercial PV panel is constructed from a number of PV cells. A PV cell is constructed from a p-n homo – junction material. The homo – junction is a semiconductor interface that occurs between layers of similar semiconductor material. These materials have equal band gaps and they typically have different doping (semiconductor) which there is a built in electric field. The absorption of photons of energy generates DC power.

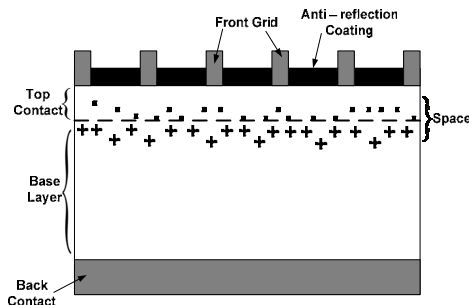


Figure 2: DC Power Generation in a PV cell.

The cross – section of a PV cell is shown in figure 2. The most common material used in PV

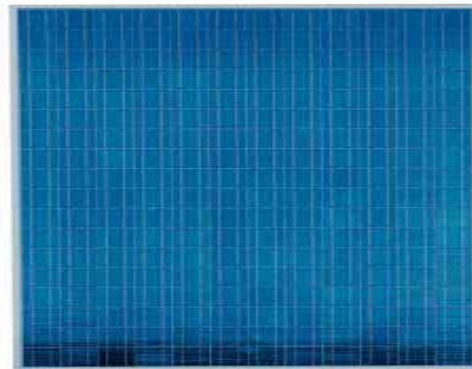


Figure3: Picture of PV module [13]



Figure 4: ASE-300-DGF/50 diode housing with bypass diodes [13].

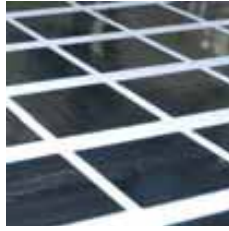


Figure 5: Full square semi-crystalline EFG cells. The electrical data applies to standard test conditions (STC): Irradiance at the module level of 1,000 W/m² with spectrum AM 1.5 and a cell temperature of 25°C.

Table 1: Electrical data [13]

Power (max.)	P _p (watts)	280 W	290 W	300 W	310 W	320 W
Voltage at maximum-power point	V _p (volts)	49.6 V	50.1 V	50.6 V	51.1 V	51.6 V
Current at maximum-power point	I _p (amps)	5.7 A	5.8 A	5.9 A	6.1 A	6.2 A
Open-circuit voltage	V _{oc} (volts)	61.9 V	62.5 V	63.2 V	63.8 V	64.4 V
Short-circuit current	I _{sc} (amps)	6.2 A	6.4 A	6.5 A	6.5 A	6.8 A

Table 2: Dimensions and weights [13]

Length mm (in)	1,892.3 (74.5")
Width mm (in)	1,282.7 (50.5")
Weight kg (lbs)	46.6 ± 2 kg (107 ± 5lbs)
Area	2.43 sq meters (26.13 ft sq)

Table 3: Characteristic data [13]

Solar cells per module	216
Type of solar cell	Semi-crystalline solar cells (EFG process), 10x10 cm ²
Connections	10 AWG single conductor, stranded copper with Multi-Contact connector. Junction box comes with 10 built-in bypass diodes.

4. MODELING A PV CELL

The use of equivalent electric circuits makes it possible to model characteristics of a PV cell. The method used here is implemented in MATLAB programs for simulations. The same modeling technique is also applicable for modeling a PV module. There are two key parameters frequently used to characterize a PV cell. Shorting together the terminals of the cell, the photon generated current will follow out of the cell as a short-circuit current (I_{sc}). Thus, I_{ph} = I_{sc}, when there is no connection to the PV cell (open-circuit), the photon generated current is shunted internally by the intrinsic p-n junction diode. This gives the open circuit voltage (V_{oc}). The PV module or cell manufacturers usually provide the values of these parameters in their datasheets [14].

The simplest model of a PV cell equivalent circuit consists of an ideal current source in parallel with an ideal diode. The current source represents the current generated by photons (often denoted as I_{ph} or I_L), and its output is constant under constant temperature and constant incident radiation of light.

The PV panel is usually represented by the single exponential model or the double exponential model. The single exponential model is shown in fig. 6. The current is expressed in terms of voltage, current and temperature as shown in equation 1 [1].

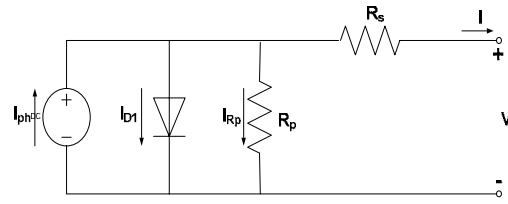


Figure 6: Single exponential model of a PV Cell.

$$I = I_{ph} - I_0 \left\{ \exp \left[\frac{q(V + IR_s)}{AkT} \right] - 1 \right\} - \frac{V + IR_s}{R_p} \quad (1)$$

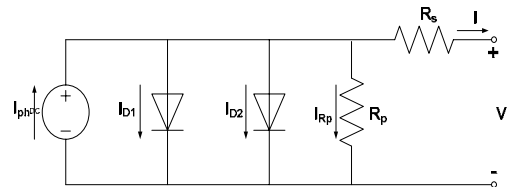


Figure 7: Double exponential model of PV Cell.

$$I = I_{ph} - I_{s1} \left\{ \exp \left[\frac{q(V + IR_s)}{AkT} \right] - 1 \right\} - I_{s2} \left\{ \exp \left[\frac{q(V + IR_s)}{AkT} \right] - 1 \right\} - \frac{V + IR_s}{R_p} \quad (2)$$

Where I_{ph}: the photo generated current; I₀: the dark saturation current; I_{s1}: saturation current due to diffusion; I_{s2}: is the saturation current due to recombination in the space charge layer; I_{Rp}: current flowing in the shunt resistance; R_s: cell series resistance; R_p: the cell (shunt) resistance; A: the diode quality factor; q: the electronic charge, 1.6 × 10⁻¹⁹ C; k: the Boltzmann's constant, 1.38 × 10⁻²³ J/K; and T: the ambient temperature, in Kelvin.

Eq.1 and Eq.2 are both nonlinear. Furthermore, the parameters (I_{ph}, I_{s1}, I_{s2}, R_s, R_{sh} and A) vary with temperature, irradiance and depend on manufacturing tolerance as shown in figure 8. Numerical methods and curve fitting can be used to estimate [1], [14].

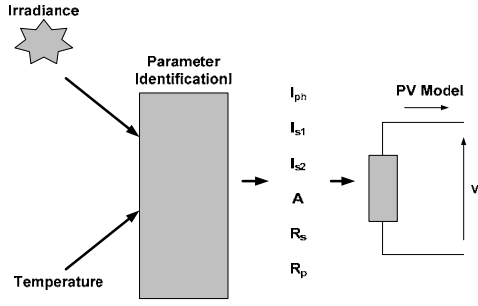


Figure 8: Modeling of a PV Panel[1]

There are three key operating points on the IV curve of a photovoltaic cell. They are the short circuit point, maximum power point and the open circuit point. At the open – circuit point on the IV curve, $V = V_{oc}$ and $I = 0$. After substituting these values in the single exponential equation (1) the equation can be obtained [1].

$$0 = I_{ph} - I_o \left\{ \exp \left[\frac{qV_{oc}}{AkT} \right] - 1 \right\} - \frac{V_{oc}}{R_p} \quad (3)$$

At the short – circuit point on the IV curve, $I = I_{sc}$ and $V = 0$. Similarly, using equation (1), we can obtain.

$$I_{sc} = I_{ph} - I_o \left\{ \exp \left[\frac{qI_{sc}R_s}{AkT} \right] - 1 \right\} - \frac{I_{sc}R_s}{R_p} \quad (4)$$

At the maximum – power point of the IV curve, we have $I = I_{mpp}$ and $V = V_{mpp}$. We can use these values to obtain the following:

$$I_{mpp} = I_{ph} - I_o \left\{ \exp \left[\frac{q(V_{mpp} + I_{mpp}R_s)}{AkT} \right] - 1 \right\} - \frac{V_{mpp} + I_{mpp}R_s}{R_p} \quad (5)$$

The power transferred to the load can be expressed as

$$P = IV \quad (6)$$

We can estimate the diode quality factor as:

$$A = \frac{V_{mpp} + I_{mpp}R_{so} - V_{oc}}{V_T \left\{ \ln \left(I_{sc} - \frac{V_{mpp}}{R_{sho}} - I_{mpp} \right) - \ln \left(I_{sc} - \frac{V_{oc}}{R_o} \right) + \frac{I_{mpp}}{I_{sc} - (V_{oc}/R_{so})} \right\}} \quad (7)$$

And

$$R_p = R_{sho} \quad (8)$$

$$I_o = \left(I_{sc} - \frac{V_{oc}}{R_p} \right) \cdot \exp \left(- \frac{V_{oc}}{AV_T} \right) \quad (9)$$

$$R_s = R_{so} - \frac{AV_T}{I_o} \cdot \exp \left(- \frac{V_{oc}}{AV_T} \right) \quad (10)$$

$$I_{ph} = I_{sc} \left(1 + \frac{R_s}{R_p} \right) + I_o \left(\exp \frac{I_{sc}R_s}{AV_T} - 1 \right) \quad (11)$$

As a very good approximation, the photon generated current, which is equal to I_{sc} , is directly proportional to the irradiance, the intensity of illumination, to PV cell [15]. Thus, if the value, I_{sc} , is known from the datasheet, under the standard test condition, $G_o=1000W/m^2$ at the air mass (AM) = 1.5, then the photon generated current at any other irradiance, G (W/m^2), is given by:

$$I_{sc|G} = \left(\frac{G}{G_o} \right) I_{sc|G_o} \quad (12)$$

It should be notified that, in a practical PV cell, there is a series of resistance in a current path through the semiconductor material, the metal grid, contacts, and current collecting bus [16]. These resistive losses are lumped together as a series resistor (R_s). Its effect becomes very conspicuous in a PV module that consists of many series-connected cells, and the value of resistance is multiplied by the number of cells. Shunt resistance is a loss associated with a small leakage of current through a resistive path in parallel with the intrinsic device [16]. This can be represented by a parallel resistor (R_p). Its effect is much less conspicuous in a PV module compared to the series resistance so it may be ignored [16] [17]. The ideality factor denoted as A and takes the value between one and two (as to reach the nominated characteristics) [17].

5. PHOTOVOLTAIC MODULE MODELING

A single PV cell produces an output voltage less than 1V, thus a number of PV cells are connected in series to achieve a desired output voltage. When series-connected cells are placed in a frame, it is called as a module. When the PV cells are wired together in series, the current output is the same as the single cell, but the voltage output is the sum of each cell voltage. Also, multiple modules can be wired together in series or parallel to deliver the voltage and current level needed. The group of modules is called an array. The panel construction provides protection for individual cells from water, dust etc, as the solar cells are placed into an encapsulation of flat glass. Our case here depicts a typical connection of 216 cells that are connected in series [13]. The strategy of modeling a PV module is no different from modeling a PV cell. It uses the same PV cell model. The parameters are the all same, but only a voltage parameter (such as the open-circuit voltage) is different and must be divided by the number of cells. An electric model with moderate complexity [18] is shown in figure 9, and provides fairly accurate results. The model consists of a current source (I_{sc}), a diode (D), and a

series resistance (R_s). The effect of parallel resistance (R_p) is very small in a single module, thus the model does not include it. To make a better model, it also includes temperature effects on the short-circuit current (I_{sc}) and the reverse saturation current of diode (I_o). It uses a single diode with the diode ideality factor set to achieve the best $I-V$ curve match.

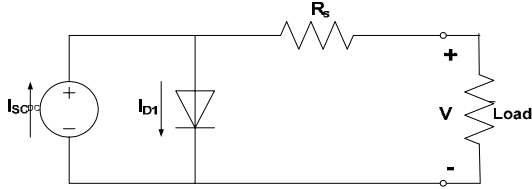


Figure9: Equivalent circuit used in the simulations
The equation (13) describes the current-voltage relationship of the PV cell.

$$I = I_{sc} - I_o \left(\exp\left(q \left(\frac{V + IR_s}{AkT} \right) \right) - 1 \right) \quad (13)$$

Where: I is the cell current (the same as the module current); V is the cell voltage = {module voltage} ÷ {No. of cells in series}; T is the cell temperature in Kelvin (K).

First, calculate the short-circuit current (I_{sc}) at a given cell temperature (T):

$$I_{sc|T} = I_{sc|T_{ref}} [1 + a(T - T_{ref})] \quad (14)$$

Where: I_{sc} at T_{ref} is given in the datasheet (measured under irradiance of $1000W/m^2$), T_{ref} is the reference temperature of PV cell in Kelvin (K), usually $298K$ ($25^\circ C$), a is the temperature coefficient of I_{sc} in percent change per degree temperature also given in the datasheet.

The short-circuit current (I_{sc}) is proportional to the intensity of irradiance, thus I_{sc} at a given irradiance (G) is introduced by Eq. 12.

The reverse saturation current of diode (I_o) at the reference temperature (T_{ref}) is given by the equation (15) with the diode ideality factor added:

$$I_o = \frac{I_{sc}}{\left(\exp\left(\frac{qV_{oc}}{AkT} \right) - 1 \right)} \quad (15)$$

The reverse saturation current (I_o) is temperature dependant and the I_o at a given temperature (T) is calculated by the following equation [18].

$$I_{o|T} = I_{o|T_{ref}} \left(\frac{T}{T_{ref}} \right)^{\frac{3}{A}} \exp\left(\frac{-qE_g}{Ak} \left(\frac{1}{T_{ref}} - \frac{1}{T} \right) \right) \quad (16)$$

The diode ideality factor (A) is unknown and must be estimated. It takes a value between one and two; however, the more accurate value is estimated by curve fitting [18] also, it can be estimated by try

and error until accurate value achieved. E_g is the Band gap energy (1.12 V (Si); 1.42 (GaAs); 1.5 (CdTe); 1.75 (amorphous Si)).

The series resistance (R_s) of the PV module has a large impact on the slope of the $I-V$ curve near the open-circuit voltage (V_{oc}), hence the value of R_s is calculated by evaluating the slope dI/dV of the $I-V$ curve at the V_{oc} [18]. The equation for R_s is derived by differentiating the $I-V$ equation and then rearranging it in terms of R_s as introduced in equation (17).

$$R_s = - \frac{dV}{dI} \Big|_{V_{oc}} - \frac{AkT / q}{I_o \exp\left(\frac{qV_{oc}}{AkT} \right)} \quad (17)$$

Where: $\frac{dV}{dI} \Big|_{V_{oc}}$ is the slope of the $I-V$ curve at the V_{oc} (using the $I-V$ curve in the datasheet then divide it by the number of cells in series); V_{oc} is the open-circuit voltage of cell (Dividing V_{oc} in the datasheet by the number of cells in series).

Finally, the equation of $I-V$ characteristics is solved using the Newton's method for rapid convergence of the answer, because the solution of current is recursive by inclusion of a series resistance in the model [18]. The Newton's method is described as:

$$x_{n+1} = x_n - \frac{f(x_n)}{f'(x_n)} \quad (18)$$

Where: $f'(x)$ is the derivative of the function, $f(x) = 0$, x_n is a present value, and x_{n+1} is a next value.

$$f(I) = I_{sc} - I - I_o \left(\exp\left(q \left(\frac{V + IR_s}{AkT} \right) \right) - 1 \right) = 0 \quad (19)$$

By using the above equations the following output current (I) is computed iteratively.

$$I_{n+1} = I_n - \frac{I_{sc} - I_n - I_o \left(\exp\left(q \left(\frac{V + I_n R_s}{AkT} \right) \right) - 1 \right)}{-1 - I_o \left(\frac{qR_s}{AkT} \right) \exp\left(q \left(\frac{V + I_n R_s}{AkT} \right) \right)} \quad (20)$$

6. SIMULATION RESULTS

The figures of $I-V$ characteristics at various module temperatures are simulated with the MATLAB model for our PV module are shown. Also, the $P-V$ relations at various module temperatures are presented. All of these are done at various irradiance values are introduced.

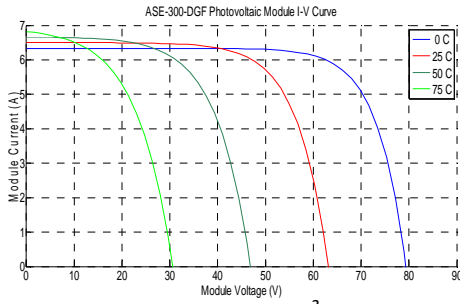


Figure 10: I-V curves at (1KW/m²; 0, 25, 50, 75°C)

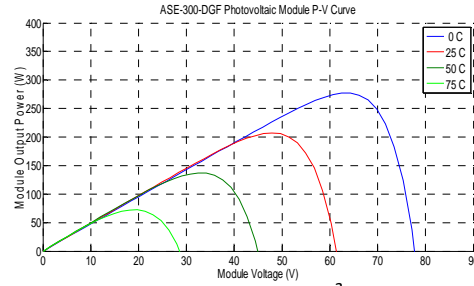


Figure 15: P-V curves (0.75KW/m²; 0, 25, 50, 75°C)

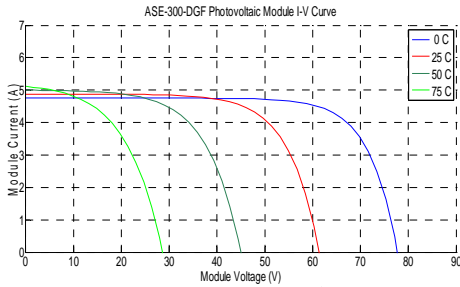


Figure 11: I-V curves (0.75 KW/m²; 0, 25, 50, 75°C)

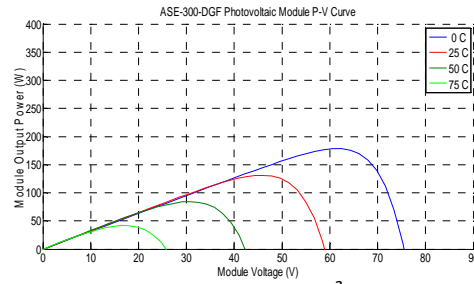


Figure 16: P-V curves (0.50KW/m²; 0, 25, 50, 75°C)

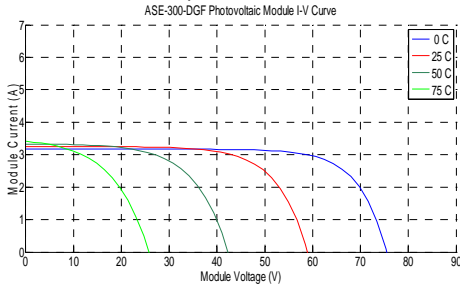


Figure 12: I-V curves (0.50 KW/m²; 0, 25, 50, 75°C)

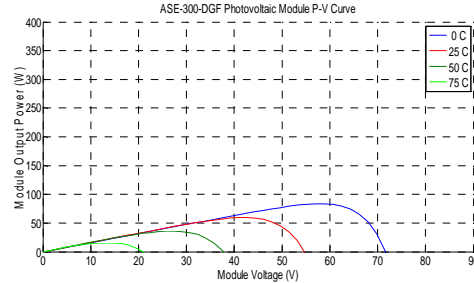


Figure 17: P-V curves (0.25KW/m²; 0, 25, 50, 75°C)

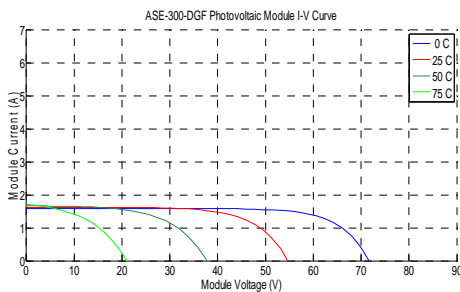


Figure 13: I-V curves (0.25 KW/m²; 0, 25, 50, 75°C)

Finally, a set of 3 D figures are proposed to cover the most probable situations at various irradiance, various temperature with the current, the voltage, and the power. These surface faces relations will be considered later as the learning or training data for the general neural network simulation.

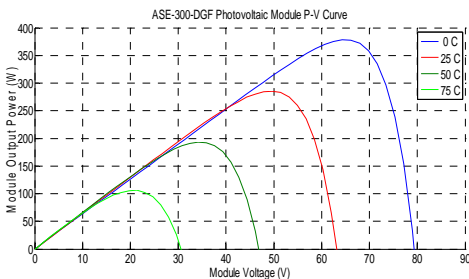


Figure 14: P-V curves at (1KW/m²; 0, 25, 50, 75°C)

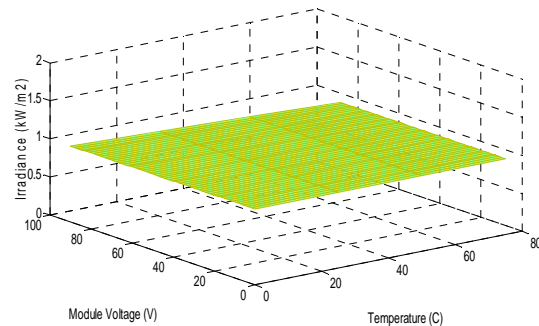


Figure 18: Voltage & Temp. & (1KW/m²) Irradiance

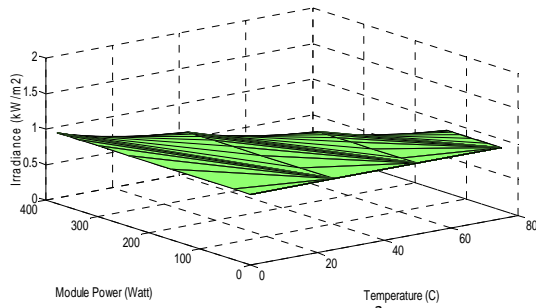


Figure 19: Power & Temp.&(1KW/m²) Irradiance

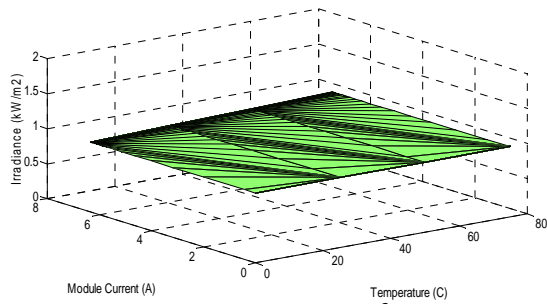


Figure 20: Current & Temp.&(1KW/m²) Irradiance

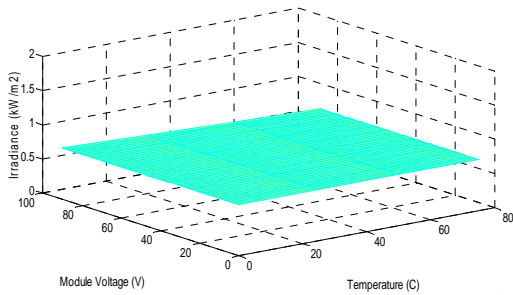


Figure 21: Voltage & Temperature&(0.75KW/m²)

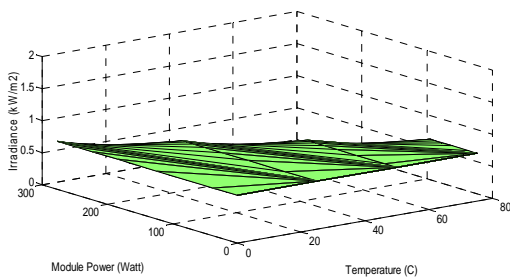


Figure 22: Power & Temperature&(0.75KW/m²)

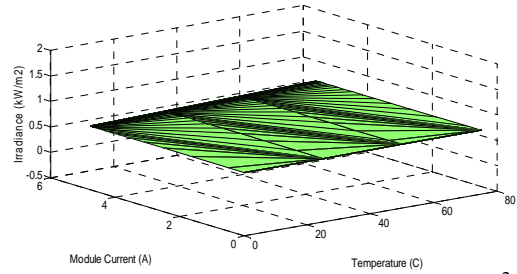


Figure 23: Current & Temperature&(0.75KW/m²)

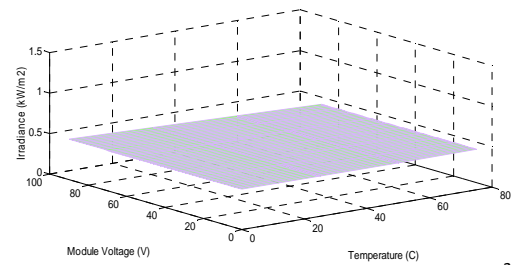


Figure 24: Voltage & Temperature&(0.50KW/m²)

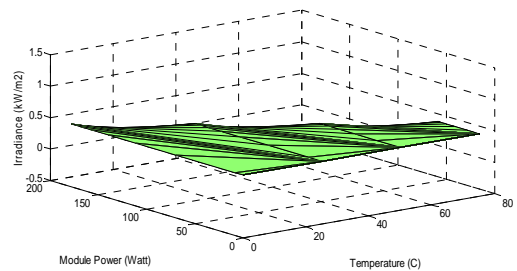


Figure 25: Power & Temperature&(0.50KW/m²)

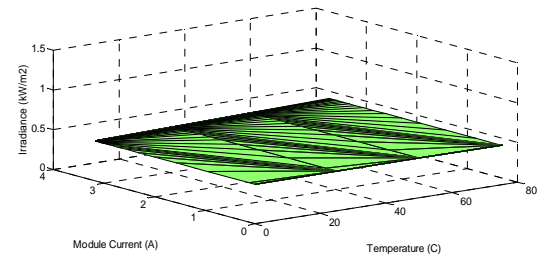


Figure 26: Current & Temperature&(0.50KW/m²)

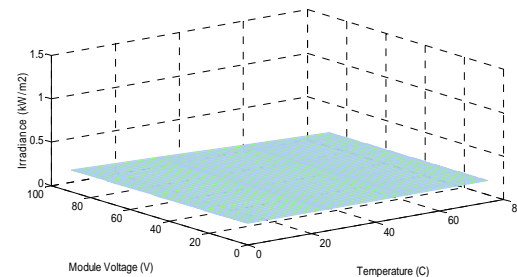


Figure 27: Voltage & Temperature&(0.25KW/m²)

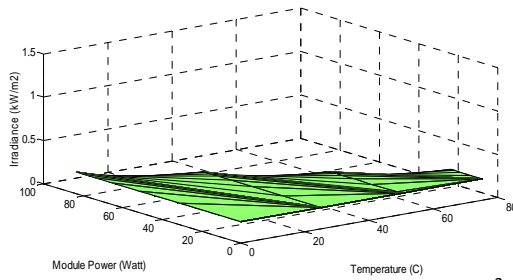


Figure 28: Power & Temperature & (0.25KW/m²)

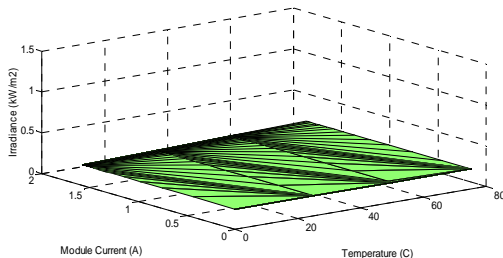


Figure 29: Current & Temperature & (0.25KW/m²)

The neural network has the ability to deal with all previous relations as surface or mapping face, due to this technique ability for interpolation between points with each other and also curves.

7. ARTIFICIAL NEURAL NETWORKS (ANNS) TECHNIQUE

An ANN consists of very simple and highly interconnected processors called neurons. The neurons are connected to each other by weighted links over which signals can pass. Each neuron receives multiple inputs from other neurons in proportion to their connection weights and generates a single output which may propagate to several other neurons [19]. Among the various kinds of ANNs that exist, the Back-propagation learning algorithm has become the most popular used method in engineering application. It can be applied to any feed-forward network with differentiable activation functions [20], and it is the type of network used in this paper.

A. Fundamentals of Neural Network

The ANN modeling is carried out in two steps; the first step is to train the network, whereas the second step is to test the network with data, which were not used for training. It is important that all the information the network needs to learn is supplied to the network as a data set. When each pattern is read, the network uses the input data to

produce an output, which is then compared to the training pattern. If there is a difference, the connection weights are altered in such a direction that the error is decreased. After the network has run through all the input patterns, if the error is still greater than the maximum desired tolerance, the ANN runs through all the input patterns repeatedly until all the errors are within the required tolerance [21], [22].

B. Data Collection, Analysis and Processing

Quality, availability, reliability, repeatability, and relevance of the data used to develop and run the system is critical to its success. Data processing starts from the data collections and analysis followed by pre-processing and then feeds to the neural network.

C. Network Structure Design

Though theoretically there exists a network that can simulate a problem to any accuracy, there is no easy way to find it. To define an exact network architecture such as how many hidden layers should be used, how many units should there be within a hidden layer for a certain problem is a painful job.

1) Number of Hidden Layers

Because networks with two hidden layers can represent functions with any kind of shapes, there is no theoretical reason to use networks with more than two hidden layers. In general, it is strongly recommended that one hidden layer be the first choice for any feed-forward network design [19-22].

2) Number of Hidden Units (node)

Another important issue in designing a network is how many units to place in each layer. Using too few units can fail to detect the signals fully in a complicated data set, leading to under fitting. Using too many units will increase the training time, perhaps so much that it becomes impossible to train it adequately in a reasonable period of time. The best number of hidden units depends on many factors – the numbers of input and output units, the number of training cases, the amount of noise in the targets, the complexity of the error function, the network architecture, and the training algorithm. The best approach to find the optimal number of hidden units is trial and error.



3) *Initializing Back-Propagation feed-forward network*

Back-propagation is the most commonly used method for training multi-layer feed-forward networks. For most networks, the learning process is based on a suitable error function, which is then minimized with respect to the weights and bias. The algorithm for evaluating the derivative of the error function is known as back-propagation, because it propagates the errors backward through the network.

4) *Training the network*

Training occurs according to any training function as previous and we must decide the training parameters with their default values: The order used for training is for example $[net, tr] = \text{train}(net, pn, tn)$ where pn, tn is the input and output which are normalized

5) *Network simulation*

To obtain the output of the network, we must simulate it the order, which can be used, is $an = \text{sim}(net, pn)$; where an : is the network but normalized so if we want to un - normalize it we use this order $a = \text{poststd}(an, meant, stdt)$. To Performs a linear regression between the network response the target, and computes the correlation coefficient use the order $(R \text{ value between the network response and the target})$. $[m, b, r] = \text{postreg}(a, t)$ [Matlab\ toolbox]; where a, t are the network output and desired or actual output and returns, M - Slope of the linear regression; B - Y intercept of the linear regression; R - Regression R -value. $R=1$ means perfect correlation.

6) *Weights and Bias*

The weights and bias, can be obtained from training data by the orders; $\text{Net.iw}\{1, 1\}$...for the weight from input layer to hidden layer; $\text{Net.}\{b1\}$ bias to a hidden layer $\text{Net.lw}\{2, 1\}$...for the weight from hidden layer to output layer; $\text{Net.}\{b2\}$... bias to output layer from a hidden layer

7) *Testing the network*

At first the data for testing mainly the input and the output from the network is prepared and then is compared with the desired or actual output to test

the ability of the network by using the same initialized network.

$[p1n, meanp1, stdp1, t1n, meant1, stdt1] = \text{prestd}(p1, t1)$

$net = \text{train}(net, p1n)$; $an1 = \text{sim}(net, p1)$; $[a1] = \text{poststd}(an1, meant1, stdt1)$; $[m, b, r] = \text{postreg}(a1, t1)$

where: $p1, t1$ are testing data, $an1$: is normalized output, $a1$: un- normalized output

8) *Derived mathematical equations*

Finally mathematical equations can be derived [23], in order to be used in future to calculate the output from the input data without needing to construct a neural network by using the weights and bias according to activation and transfer functions as when using $\{\text{logsig 'purelin}\}$ as in this paper, the next sequences have to be followed

1- Normalize the input data as shown previous .

2- Calculate sum of $x_i * w_{\{i, j\}} + b_{\{i\}} = h_i$ for each node in hidden layer

where: x_i : is the input variable, h_i : is a hidden layer input from input layer $w_{\{i, j\}}$, $b_{\{i\}}$ are obtained before, $\text{Net.iw}\{1,1\}$ $\text{Net.b}\{1\}$

3- Calculate the output from each node in hidden layer to output layer (F_i) according to transfer function here is logsig so $F_i = 1/(1+\exp(-h_i))$

4- Calculate the sum of output from hidden layer to output layer $h_i = F_i * \text{Net.lw}\{2,1\} + \text{Net.b}\{2\}$

5- Calculate the required output according to transfer fun. here is purelin [Matlab/toolbox] so output

$(y_i) = h_i$ according to number of the required outputs

6- Un normalized y to obtain the output $= y * \text{stdt} + \text{meant}$...to obtain the actual values

8. ANN PV MODULE MODEL WITH ITS REGRESSION FUNCTION

This model uses the previous technique which used and verified before in the field of renewable energy like in [24-27]. This model uses the previous 3D graphs illustrated before as training or learning data for input and desired target. The inputs in this model are the Irradiance and Temperature; the outputs are: Module Voltage, Current, and Power. This model with its hidden and output layers' suitable neurons numbers is depicted in figure 30. Also, the general neural network, and training state are presented in figures 31, and 32 respectively.

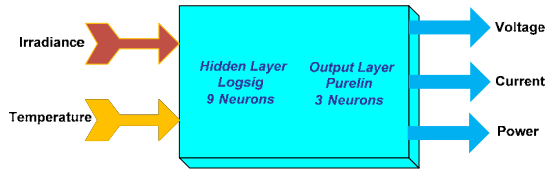


Figure 30: ANN PV Cell Module Model

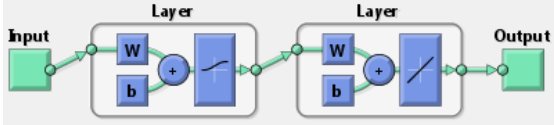


Figure 31: Neural Network

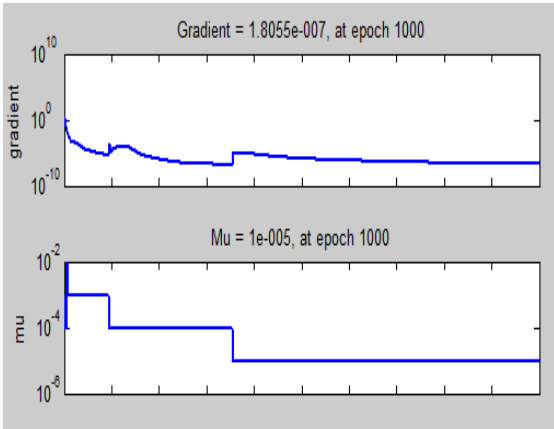


Figure 32: Training State

The normalized inputs G_n : (Normalized Irradiance); T_n : (Normalized Temperature) are as follow:

$$G_n = (G - 0.6250) / (0.2797) \quad (21)$$

$$T_n = (T - 37.5000) / (27.9683) \quad (22)$$

Equations (21) and (22) present the normalized inputs for irradiance and temperature, also the following equations lead to the required derived outputs equations.

$$E1 = -0.3884G_n - 0.8968T_n + 2.8411 \quad (23)$$

$$F1 = 1 / (1 + \exp(-E1))$$

$$E2 = 10.8336G_n - 0.1120T_n - 4.7062 \quad (24)$$

$$F2 = 1 / (1 + \exp(-E2))$$

$$E3 = -0.3773G_n - 9.6071T_n + 7.2495 \quad (25)$$

$$F3 = 1 / (1 + \exp(-E3))$$

$$E4 = -0.0696G_n - 9.4705T_n - 5.0369 \quad (26)$$

$$F4 = 1 / (1 + \exp(-E4))$$

$$E5 = 6.3252G_n + 0.3523T_n + 4.6963 \quad (27)$$

$$F5 = 1 / (1 + \exp(-E5))$$

$$E6 = -0.1062G_n + 3.4660T_n + 8.7149 \quad (28)$$

$$F6 = 1 / (1 + \exp(-E6))$$

$$E7 = 0.1802G_n + 4.0327T_n + 3.7157 \quad (29)$$

$$F7 = 1 / (1 + \exp(-E7))$$

$$E8 = 11.6503G_n - 1.1094T_n + 11.1433 \quad (30)$$

$$F8 = 1 / (1 + \exp(-E8))$$

$$E9 = 0.2372G_n - 0.8735T_n + 0.7613 \quad (31)$$

$$F9 = 1 / (1 + \exp(-E9))$$

The normalized outputs are:

$$V_n = .0466 F1 + .0080 F2 + .0661 F3 - .2311 F4 - .0071 F5 + 2.5608 F6 + 0.0771 F7 + 0.0091 F8 - 0.0217 F9 - 2.7656 \quad (32)$$

$$I_n = 6.2907 F1 + 1.5501 F2 + 0.2881 F3 + 1.8330 F4 - 1.1986 F5 - 0.6123 F6 - 1.2526 F7 + 1.6547 F8 - 2.6831 F9 - 6.1682 \quad (33)$$

$$P_n = 7.2249 F1 + 1.7820 F2 + 1.0262 F3 + 5.1377 F4 - 1.3507 F5 - 0.9574 F6 + 3.4515 F7 + 1.8830 F8 - 6.9036 F9 - 7.3615 \quad (34)$$

The un- normalized out puts

$$V = 25.2226 V_n + 42.6563 \quad (35)$$

$$I = 2.1788 I_n + 2.3181 \quad (36)$$

$$P = 57.5303 P_n + 81.4030 \quad (37)$$

9. CONCLUSIONS

This paper presents a simple but efficient photovoltaic modeling trial for both specific and general one. It models each component and simulates them using MATLAB. The result shows that the PV model using the equivalent circuit in moderate complexity provides good matching with the real PV module. Simulations are based on Schott ASE-300-DGF PV panel as a practical one. A non-specific modeling and simulation at more probable situations for variable values of temperature and irradiance are presented. The simulation results at each irradiance value with various temperature values and corresponding characteristics are well depicted in 3-D figures. ANN is used for the proposed range of irradiance and temperature as model inputs, with the corresponding values of voltages, currents, and power as outputs with its algebraic equations. This neural network unit is implemented, using the back propagation (BP) learning algorithm due to its



benefits to have the ability to predict values in – between learning values, also make interpolation between learning curves data. This is done with suitable number of network layers and neurons at minimum error and precise manner.

10. ACKNOWLEDGEMENT

I would like to thank Ms. Shaza M. Abd Al Menem for her effort in this research editing.

REFERENCES:

- [1] Ali Keyhani, Mohammad N. Marwali, and Min Dai, "Integration of Green and Renewable Energy in Electric Power Systems," Wiley, January 2010
- [2] Ali Keyhani, "Cyber-Controlled Smart Microgrid Systems of the Future: The High Penetration of Renewable and Green Energy Sources", New Research Directions for Future Cyber-Physical Energy Systems, Sheraton Baltimore City Center Hotel Baltimore, Maryland, June 2009
- [3] Ali Keyhani, Jin-Woo Jung, Min Dai, "Control of Renewable Energy Sources in Smart Grid Systems," Smart Grids Africa, 28-30 July 2008, Johannesburg, South Africa
- [4] [s.n.], \Trends in photovoltaic applications. survey report of selected IEA countries between 1992 and 2006.
- [5] T. Markvart and L. Castaner, Practical Handbook of Photovoltaics, Fundamentals and Applications. Elsevier, 2003.
- [6] Larminie, J., and Dicks, A. . Fuel Cell Systems Explained, 2nd Ed., John Wiley & Sons, New York, 2003.
- [7] Shen, J. "Emerging Enabling Technologies in Vehicular Power Electronics." Proceedings of the 2004 3rd Annual Summer Workshop of the NDIA Intelligent Vehicles Symposium, 2004.
- [8] Costamagna, P., and Srinivasan, S. "Quantum jumps in the PEMFC science and technology from the 1960s to the year 2000: Part I. Fundamental scientific aspects." Journal of Power Sources, 102, pp. 242-252, 2001.
- [9] Ahluwalia, R., Wang, X., Lasher, S., Sinha, J., Yang, Y., and Sriramulu, S. "Performance of automotive fuel cell systems with nanostructured thin film catalysts." Proceedings of the 2007 Fuel Cell Seminar and Exposition, San Antonio, TX, 2007.
- [10] Meimei Guo, Baijun Liu, Long Li, Chang Liu, Lifeng Wang, Zhenhua Jiang, "Preparation of sulfonated poly(ether ether ketone)s containing amino groups/epoxy resin composite membranes and their in situ crosslinking for application in fuel cells," Journal of Power Sources 195 (2010) 11–20
- [11] Tauqir A. Sherazi, Michael D. Guiver, David Kingston, Shujaat Ahmad, M. Akram Kashmiri, Xinzhong Xue, "Radiation-grafted membranes based on polyethylene for direct methanol fuel cells," Journal of Power Sources 195 (2010) 21–29
- [12] Xiu Qing Xing, KahWai Lum, Hee Joo Poh, Yan LingWu, "Optimization of assembly clamping pressure on performance of proton-exchange membrane fuel cells," Journal of Power Sources 195 (2010) 62–68
- [13] Schott ASE-300-DGF PV panel data sheet. Source (Affordable Solar website) http://www.affordable-solar.com/admin/product_doc/Doc_pd-00-009-c_ase_300_20080328114646.pdf
- [14] Masters, Gilbert M. Renewable and Efficient Electric Power Systems John Wiley & Sons Ltd, 2004
- [15] Messenger, Roger & Jerry Ventre Photovoltaic Systems Engineering 2nd Edition CRC Press, 2003
- [16] Castañer, Luis & Santiago Silvestre Modelling Photovoltaic Systems, Using PSpice John Wiley & Sons Ltd, 2002
- [17] [Green, Martin A. Solar Cells; Operating Principles, Technology, and System Applications Prentice Hall Inc., 1982
- [18] Walker, Geoff R. "Evaluating MPPT converter topologies using a MATLAB PV model" Australasian Universities Power Engineering Conference, AUPEC '00, Brisbane, 2000
- [19] TT Chow, Zhang GQ, Lin Z, Song CL.: Global optimization of absorption chiller system by genetic algorithm and neural network. Energy Buildings 2002;34:103–9.
- [20] SA Kalogirou "Applications of artificial neural networks in energy systems: a review," Energy Convers Manage 1999; 40:1073–87.
- [21] SA. Kalogirou "Applications of artificial neural networks for energy systems," Appl Energy 2000; 67:17–35.
- [22] SA. Kalogirou "Long-term performance prediction of forced circulation solar domestic water heating Systems using artificial neural networks," Appl Energy 2000; 66:63–74.



- [23] Arzu Sencan, Kemal A. Yakut, Soteris A. Kalogirou “ Thermodynamic analysis of absorption systems using artificial neural network,” Renewable Energy, Volume 31, issue 1, Jan. 2006, pages 29 – 43.
- [24] A. El Shahat, “Generating Basic Sizing Design Regression Neural Function for HSPMSM in Aircraft” EP-127, 13th International Conference on Aerospace Science & Aviation Technology, May 26 – 28, 2009, ASAT 2009 – Military Technical College, Cairo, Egypt.
- [25] El Shahat, A and El Shewy, H, “Neural Unit for PM Synchronous Machine Performance Improvement used for Renewable Energy”, Ref: 93, The Third Ain Shams University International Conference on Environmental Engineering (Ascee- 3), April 14-16 2009, Cairo, Egypt.
- [26] A. El Shahat, and H. El Shewy, “Neural Unit for PM Synchronous Machine Performance Improvement used for Renewable Energy”, Paper Ref.: 910, Global Conference on Renewable and Energy Efficiency for Desert Regions (GCREEDER2009), Amman, Jordan.
- [27] A. El Shahat, and H. El Shewy, “PM Synchronous Motor Control Strategies with Their Neural Network Regression Functions”, Journal of Electrical Systems, Vol. 5, Issue 4, Dec. 2009.